Int. J. Appl. Ceram. Technol., 12 [5] 985–990 (2015)
DOI:10.1111/ijac.12375

Effect of Thermal Initiator Concentrations on the Structure and Optical Band Gaps of Polyvinylsilazane-Derived SiOCN Ceramics

Yan Li, Yuxi Yu,* and Haisheng San

Fujian Key Laboratory of Advanced Materials, Department of Materials Science and Engineering, College of Materials, Xiamen University, Xiamen 361005, China

Yansong Wang

Key Laboratory of Optical System Advanced Manufacturing Technology, Changchun Institute of Optics, Fine Mechanics and Physics, CAS, Changchun 130033, China

Qingkai Han

School of Mechanical Engineering, Dalian University of Technology, Dalian 116023, China

Jiyu Fang and Linan An

Department of Materials Science and Engineering and Advanced Materials Processing and Analysis Center, University of Central Florida, Orlando, Florida 32816

SiOCN ceramics are formed by the thermal decomposition of a polyvinylsilazane precursor in the presence of a dicumyl peroxide (DP) thermal initiator with different concentrations. The SiOCN ceramics pyrolyzed at 1000°C with different concentrations of DP are characterized with X-ray diffraction, transmission electron microscope, electron paramagnetic resonance, and UV-visible spectroscopy. We find that the structure and optical band gap of the SiOCN ceramics can be changed by altering the concentration of DP. There is a critical concentration, at which the structural and optical behavior varied in different ways as a function of the concentration of DP. The detailed mechanism is discussed.

Introduction

In recent years, a great deal of attentions have been devoted to amorphous silicon-based ceramics synthesized by the thermal decomposition of polymeric precursors,[1–4] beacause polymer-derived ceramics (PDCs) show excellent high-temperature properties, such as excellent high-temperature stability,[5,6] oxidation/corrosion resistance,[7,8] creep resistance,[9] high-temperature semiconducting behavior,[10–13] and high piezoresistivity.[14–17] Furthermore, by controlling processing routes, PDCs with varied sizes and morphologies such as powders, binders, fibers, and thin films can be formed, which make them useful materials in electronic/optical devices.[18,19]

It has been proposed that the conduction mechanism of PDCs is a result of the formation of a free carbon phase.[11,20] When the concentration of carbon clusters is higher than a critical value, the conduction of PDCs is controlled by a tunneling-percolation mechanism, resulting in high piezoresistivities.[13] On the other hand, when the concentration of carbon clusters is lower than the critical value, the conduction of PDCs is controlled by the matrix phase, leading to amorphous semiconducting behaviors.[14] Previous studies showed that the electric conductivity of PDCs depended not only on the nature of precursors,[2] but also the experimental condition and the concentration of thermal initiators. Wang *et al.*[13] showed that the electric conductivity of polymer-derived SiCNs made of a polysilazane was associated with the concentration of thermal initiators, which increased until the initiator concentration reached to a critical value and then decreased with the further increase of the initiator concentration.

In this study, we studied the structure and optical behavior of polymer-derived amorphous silicon oxycarbonitrides (SiOCN) obtained at 1000°C with varied concentrations of dicumyl peroxide (DP) thermal initiator. The resultant SiOCN ceramics are characterized using X-ray diffraction (XRD), high-resolution transmission electron microscope (HRTEM), electron paramagnetic resonance (EPR) and UV-Vis spectroscopy. We found that all the

*yu_heart@163.com

samples were amorphous with defects in-plane carbon clusters. Although the properties of the SiOCN are changed drastically by adding DP to their precursors, the change in the structure and optical band gap are not monotonic with the change of DP concentrations.

Experimental

Polyvinylsilazane (PVSZ) is a well-known precursor in the synthesis of SiOCN ceramics with ~70 wt% yield.[21,22] The SiOCN ceramics studied here were synthesized using PVSZ (Mw = 500 g/mol) and DP (Sigma-Aldrich, St. Louis, MO) as a ceramic precursor and a thermal initiator, respectively. The liquid PVSZ was first mixed with different concentrations of DP. The mixture was then thermally treated in nitrogen to form a solid precursor. The detailed conditions, including PVSZ-to-DP ratio, solidification temperature and time, are shown in Table I. The resultant solid was crushed into fine powders with diameters of ~1 μm by high-energy ball milling, followed by pyrolyzing at 1000°C for 4 h in a tube furnace under flowing of ultrahigh-purity nitrogen.

The morphologies and structure properties of samples were investigated using XRD (X'pert PRO, PANalytical B.V., Almelo, the Netherlands) and HRTEM (JEM-2100; JEOL, Tokyo, Japan). XRD data were digitally recorded in a continuous scan mode in the angle (2θ) range of 15–85° at a scanning rate of 0.12°/s. EPR spectra (EMX-10/12; Bruker, Karlsruhe, Germany) were obtained using X Band Bruker EMX spectrometer operating at 9.6 GHz with a magnetic modulation of 100 kHz and 5×10^{-4} T at room temperature. The EPR spectra were processed with Bruker WIN-EPR software. The mass of the samples for EPR experiment is 7 mg.

UV-visible absorption data were recorded using Cary-5000 (230–2500 nm; Varian, Palo Alto, CA). KBr was taken as a reference material. SiOCN powders were mixed with KBr powders and then pressed into disks. The ratio of the SiOCN powder to the KBr powder was controlled so that the overall absorbance of the disks ranged between 0.1 and 0.8 to optimize the results. To remove the signal from KBr, a pure KBr disk with the same size was prepared and measured, and the result is then used as the corrected baseline. After measuring of the KBr disk, the absorption spectra of the KBr/SiOCN samples were obtained, and the absorption spectra of the pure SiOCN sample were obtained.

Results and Discussion

To obtain the information of morphologies and structure properties, the pyrolyzed samples were characterized using XRD and HRTEM. Figure 1a shows a typical XRD pattern obtained from the sample DP-6. The pattern is absence of any diffraction peaks (only a steamed buns peak is for SiO_2), suggesting the amorphous nature of the sample. The HRTEM image of the same sample also reveals no crystalline structure (Fig. 1b). The amorphous nature of the sample is further confirmed by the selected area electron diffraction (SAED) (the inset in Fig. 1b), which shows a diffuse ring pattern. All samples exhibited the similar XRD and HRTEM results, suggesting that they are all amorphous with carbon cluster regardless of DP concentrations, which are not shown in this article.

Although the optical band gap (E_{opt}) obtained from optical absorption methods is less narrow than the band gap from current conduction experiments for amorphous semiconductors, optical absorption is an useful method to study the electronic structure of materials.[23–25] Therefore, we use optical absorption methods to detect the electronic structure evolution in the SiOCN ceramic with the difference concentration ratios of thermal initiator DP. Figure 2 shows the dependence of absorption coefficient (α) on the incident photo energy at room temperature for five SiOCN samples. It is clear that all the samples have a strong absorption in UV-visible region. All the optical absorption coefficients increase rapidly with the increase of photon energy up to 4.0 eV, and the sharp increase range is defined as the mobility edge.

To obtain useful information about the electronic structures, these spectra are compared with a theoretical

Table I. Precursor, Solidification Conditions and Compositions of the SiOCN Ceramics

Samples	PVSZ-to-DP ratio	Cross-linking condition	Compositions	Apparent formula
DP-0	100:0	180°C, 1.0 h, N_2	$SiO_{0.60}C_{1.21}N_{0.41}$	$0.10Si_3N_4{\cdot}0.30SiO_2{\cdot}0.39SiC{\cdot}0.81C$
DP-2	100:2	160°C, 1.0 h, N_2	$SiO_{0.53}C_{1.17}N_{0.43}$	$0.11Si_3N_4{\cdot}0.27SiO_2{\cdot}0.41SiC{\cdot}0.76C$
DP-4	100:4	140°C, 1.0 h, N_2	$SiO_{0.57}C_{1.24}N_{0.4}$	$0.10Si_3N_4{\cdot}0.29SiO_2{\cdot}0.42SiC{\cdot}0.83C$
DP-6	100:6	140°C, 1.0 h, N_2	$SiO_{0.54}C_{1.26}N_{0.39}$	$0.08Si_3N_4{\cdot}0.27SiO_2{\cdot}0.44SiC{\cdot}0.82C$
DP-10	100:10	140°C, 1.0 h, N_2	$SiO_{0.54}C_{1.26}N_{0.42}$	$0.12Si_3N_4{\cdot}0.27SiO_2{\cdot}0.42SiC{\cdot}0.85C$

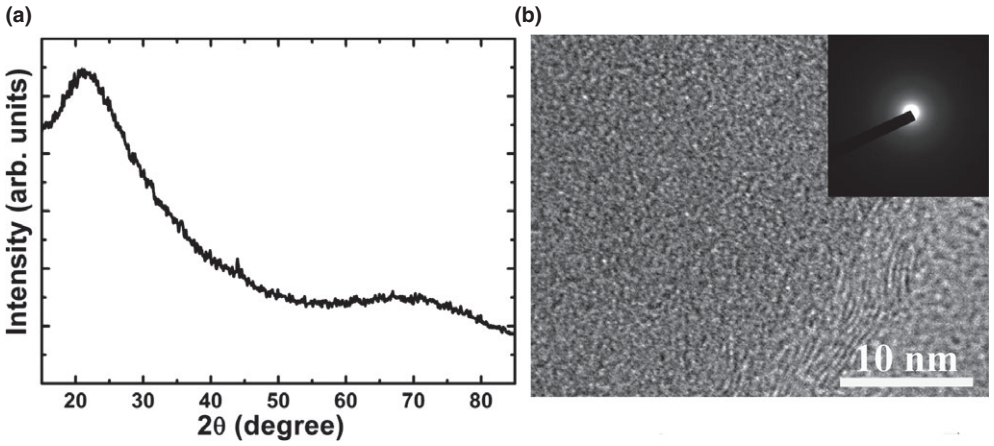

Fig. 1. (a) XRD pattern and (b) TEM micrograph of the DP-6. The SAED pattern is inset in (b).

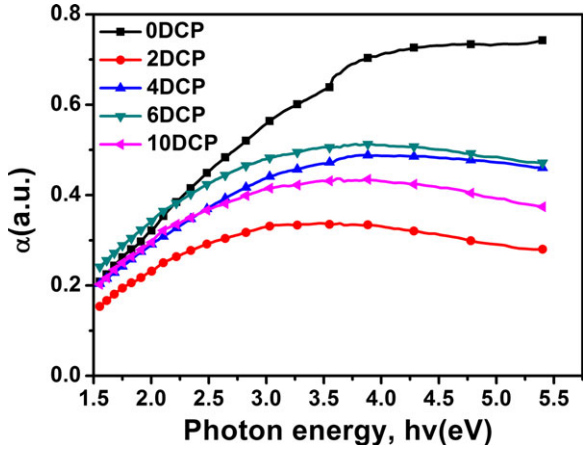

Fig. 2. Room-temperature optical absorption spectra of PVSZ pyrolyzed at 1000 °C with different amounts of DP.

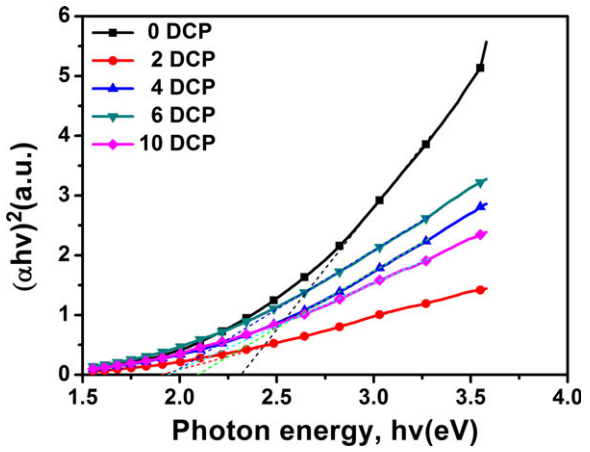

Fig. 3. Plots $(\alpha h\nu)^2$ as a function of photon energy ($h\nu$) for PVSZ pyrolyzed at 1000 °C with different amounts of DP.

model proposed by Davis and Mott[26], in which the absorbance of an amorphous semiconductor as a function of photon energy ($h\nu$) follows the equation in higher photon energy regions:

$$(\alpha h\nu)^r \propto (h\nu - E_{opt}) \quad (1)$$

where α is the absorption coefficient, $h\nu$ is the photon energy, E_{opt} is the optical band gap, and r is the exponent, which can be 1/3, 1/2, 2/3, 1, and 2, depending on the transition type in the K space.[23] It can be seen that the absorption at the excitation photon energy range of 2.5–4 eV can be described by Eq. (1) with $r = 2$, so in this range, the dependence of the absorption coefficient on photon energy can be described as:[23,26]

$$(\alpha h\nu)^2 = \mathrm{B}(h\nu - E_{opt}) \quad (2)$$

where B is a constant. Figure 3 shows $(\alpha h\nu)^2$ as a function of photon energy ($h\nu$) for the five SiOCN samples, The linear relationship obtained at higher photon energy regions suggest that the absorptions are due to the transition between the two delocalized bands. The E_{opt} is defined as the energy at which the dash line extrapolated from the straight part of the plot intersects the horizontal (energy) axis (indicated by the dotted lines in Fig. 3 and summarized in Table II). The obtained E_{opt} for the samples DP-0, DP-2, DP-4, DP-6, DP-10 are 2.32, 1.90, 2.09, 1.95, 1.94 eV (Table II), respectively.

The changes of E_{opt} should be a result of the changes of SiOCN structures. It has been shown that the E_{opt} of polymer-derived ceramics depends on their compositions and processing conditions. The obtained SiOCN ceramics are composed of amorphous Si_3N_4, amorphous SiO_2, amorphous SiC and free carbon

Table II. Curve Fit Parameters for the Five SiOCN Ceramics

Samples	0.5–1.5 eV		2–4 eV
	m	E_T	E_{opt}
DP-0	1.57 ± 0.03	0.36 ± 0.02	2.32 ± 0.01
DP-2	1.66 ± 0.08	0.44 ± 0.01	1.90 ± 0.05
DP-4	1.54 ± 0.02	0.32 ± 0.005	2.09 ± 0.03
DP-6	1.52 ± 0.03	0.22 ± 0.03	1.95 ± 0.02
DP-10	1.59 ± 0.05	0.26 ± 0.02	1.94 ± 0.01

(Table I). The content of the Si_3N_4, SiO_2, SiC and free carbon is oscillated with the concentration ratio of DP. It is known that the replacement of weaker Si-Si bonds by stronger Si-C bonds and Si-O bonds can lead to the increase of E_{opt}.[27] For pure PVSZ, the reaction between the vinyl groups and C-H bonds occurs at higher temperatures, resulting in the highest formation of Si-O and the lowest formation of Si-C. When the initiator is mixed with PVSZ, the radical-induced polymerization process occurs at lower temperatures, leading to the formation of Si-O and Si-C (shown in Table I). The total moles of SiO_2 and SiC in the amorphous matrix for the sample DP-2 which is the lowest in the samples cause the decrease of the C/Si ratio and O/Si ratio in the SiOCN matrix, resulting in the decrease of its E_{opt}.

It can be seen from Fig. 3 that at low excitation energy end the absorption coefficient is not zero, suggesting that there should be other absorption mechanisms at the excitation energy range below the band gap. Tauc and colleagues suggested that for amorphous semiconductors, the optical absorption spectra at a lower excitation energy range should follow:[23,27]

$$\alpha h\nu = B(h\nu - E_T)^m \quad (3)$$

where B is a constant called the band-tailing parameter, and E_T is an energy gap. The absorption was attributed to the transition from localized states (defect states) to delocalized states (conduction/valence band). The m can either be 1.5 or 0.5, depending on the distribution of these states. According to Inkson,[28] the m should be 1.5 for a nonallowed nonvertical transition from a deep impurity trap to a delocalized band, and the dependence of the absorption coefficient on photon energy in this range can be described as:

$$(\alpha h\nu) = B(h\nu - E_T)^{1.5} \quad (4)$$

and E_T can be calculated from the equation:

$$E_T = E_C - E_d \quad (5)$$

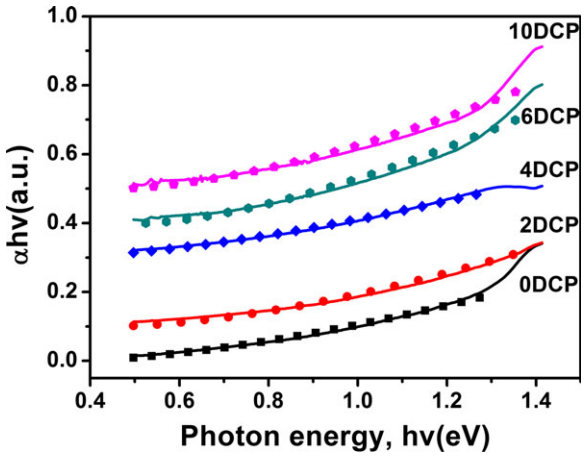

Fig. 4. Plots of αhν as a function of photon energy (hν) for PVSZ pyrolyzed at 1000 °C with different amounts of DP. The solid symbols are experiment data; the short dot lines are curve fits using Eq. (3).

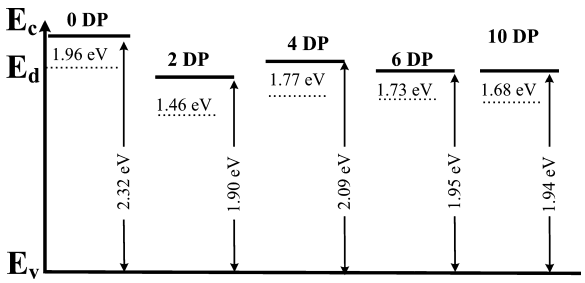

Fig. 5. The electronic structures of PVSZ pyrolyzed at 1000 °C with different amounts of DP.

where E_C is the mobility edge of extended conduction band, and E_d is a deep defect level with a high density of states. The fitting of the Eq. (4) is good over large energy range (Fig. 4 and Table II). The value of E_{opt} and E_T obtained for all SiOCN samples is given in Table II. Based on the above results, the electronic structures of the SiOCN were constructed (Fig. 5). The result reveal that the DP-2 sample has the lowest optical band gap.

As can be seen in Table II, E_d also varies as the weight proportion of DP, and consists with the concentration of the free carbon. So this phenomenon could be explained by considering dangling bands in the free carbon that have unpaired electrons as defects and generate a deep defect level within the band gap. The point defects wereanalyzed using EPR. Figure 6 shows the room-temperature EPR spectra of the five samples at X-band frequency. The spectra show only one intense line of a predominantly Lorentzian shape with a g value of 2.0012 ± 0.0002, regardless of the amount of DP. This g

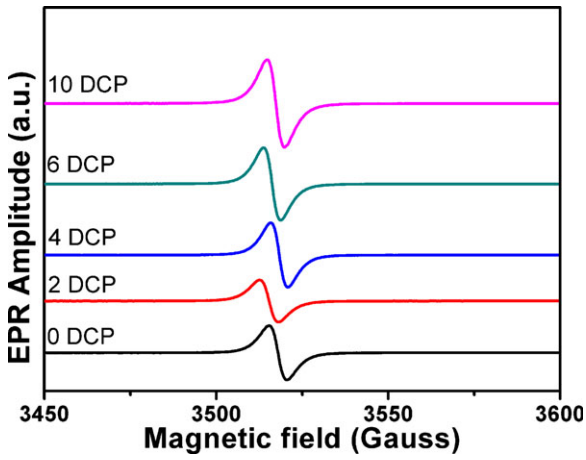

Fig. 6. EPR of PVSZ pyrolyzed at 1000 °C with different amounts of DP.

factor suggests that the observed EPR line is a result of the carbon dangling bonds (unpaired electrons) presented in the carbon-inherited spin species in graphite domains.[29–31]

The relative number of spins (n) can be roughly calculated from the spectra by the following equation:[31]

$$n = I(\Delta H_{pp})^2 \quad (6)$$

where I is the peak-to-peak intensity height and ΔH_{pp} is the peak-to-peak line width. Figure 7 shows the plots of the ΔH_{pp} and the n as a function of DP concentration. Previous studies suggested that the sp^2-hybridization is characterized by the line widths higher than 10 Gauss; while the sp^3-hybridization is characterized by the line widths lower than 10 Gauss, due to the different extents of spin delocalization within the "in-plane" dangling bonds.[32] As can be seen from Fig. 7a, the ΔH_{pp} of all samples is lower than 10 Gauss, suggesting that they contain sp^3-type carbon dangling bonds. According to Ohnishis equation:[33]

$$\Delta H_{pp} \propto l^{-\frac{1}{2}} \quad (7)$$

where l is the length of conjugated chains. It is clear that the length of the conjugated chains is determined by the concentration of the initiator, but not a monotonic relationship. We can conclude that the length of conjugated chains of SiOCN samples varies as the weight proportion of DP. For pure PVSZ, the reaction between the vinyl groups and C-H bonds occursat higher temperatures (shown in Table I), leading to the formation of short carbon conjugated chains. When the initiator is mixed with PVSZ, the radical-induced polymerization process occurs at lower temperatures (Table I), the length of the carbon conjugated chains is determined by the concentration of the initiator. The DP-2 sample has the lowest conjugated chain length, after the length of conjugated chains slight increases with the further increasing of the weight proportion of DP. The number of the spins also varies as the weight proportion of DP (Fig. 7b). The sample DP-2 has the lowest of n. The defects is derived from the "in-plane" dangling bonds in the free carbon, so the number of the defects is controlled by the length of the carbon conjugated chains as well.

Summary

A polymer-derived SiOCN ceramic has been synthesized by the pyrolyzation of PVSZ in the presence of DP with different concentrations at 1000°C. We find that the structure and optical properties of the derived SiOCN ceramics depend on the concentration of DP. There is a critical concentration of DP (2 wt%). Above the critical concentration, the optical band gap of the

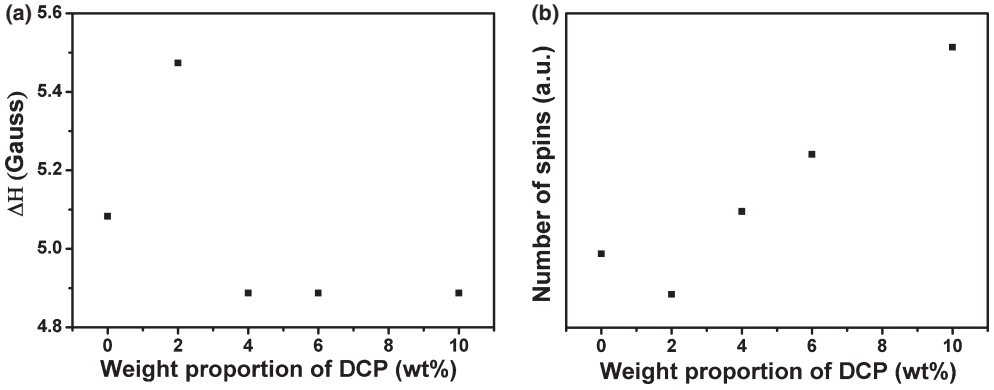

Fig. 7. ΔH_{pp} (a) and n (b) as a function of weight proportions of DP.

SiOCN ceramics increases slightly with increasing DP concentrations, and then almost keep constant, which may be caused by the replacement of weaker Si-Si bonds by stronger Si-C bonds and Si-O bonds. At the same time, the length of conjugated chains of free carbons in the free carbon chains decreases slightly with increasing DP concentrations, and the number of the defects derived from the "in-plane" dangling bonds on the free carbon decreases slightly with increasing DP concentrations, which is result in the generation of a deep defect level within the band gap. Our results show the possibility of altering the optical/electronic properties of the PDC by changing DP concentrations, which is critical for developing their applications in optical/electronic device.

Acknowledgments

Financial support from the Natural Science Foundation of China (51175444, 61274120), the Fundamental Research Funds for the Central Universities (Xiamen University, 2011121002), the Aviation Science Foundation of China (2013ZD68009), New Century Excellent Talents in Fujian Province University (2013), the Natural Science Foundation of Fujian Province of China (2014J01206), Xiamen Municipal Bureau of Science and Technology (3502Z20143009), and Shenzhen City Science and Technology Innovation Committee (JCYJ20120618155425009) is acknowledged.

References

1. R. Riedel, G. Passing, H. Schönfelde, and R. J. Brook, *Nature*, 355 [6362] 714–717 (1992).
2. P. Colombo, G. Mera, R. Riedel, and G. D. Soraru, *J. Am. Ceram. Soc.*, 93 [7] 1805–1837 (2010).
3. S. Sarkar, Z. H. Gan, L. N. An, and L. Zhai, *J. Phys. Chem. C*, 115 [50] 24993–25000 (2011).
4. G. Mera, A. Navrotsky, S. Sen, H. J. Kleebed, and R. Riedel, *J. Mater. Chem. A*, 1 3826–3836 (2013).
5. T. Varga, *et al.*, *J. Am. Ceram. Soc.*, 90 [10] 3213–3219 (2007).
6. R. Bhandavat and G. Singh, *ACS Appl. Mater. Interfaces*, 4 [10] 5092–5097 (2012).
7. K. Terauds, D. B. Marshall, and R. Raj, *J. Am. Ceram. Soc.*, 96 [4] 1278–1284 (2013).
8. Y. G. Wang, W. F. Fei, Y. Fan, L. G. Zhang, W. G. Zhang, and L. N. An, *J. Mater. Res.*, 21 [7] 1625–1628 (2006).
9. B. Papendorf, *et al.*, *J. Am. Ceram. Soc.*, 96 [1] 272–280 (2013).
10. S. Trassl, M. Puchinger, E. Rossler, and G. Ziegler, *J. Eur. Ceram. Soc.*, 23 [5] 781–789 (2003).
11. M. Graczyk-Zajac, G. Mera, J. Kaspar, and R. Riedel, *J. Eur. Ceram. Soc.*, 30 [15] 3235–3243 (2010).
12. H. Y. Ryu, Q. Wang, and R. Raj, *J. Am. Ceram. Soc.*, 93 [6] 1668–1676 (2010).
13. Y. S. Wang, *et al.*, *J. Am. Ceram. Soc.*, 91 [12] 3971–3975 (2008).
14. R. Riedel, L. Toma, E. Janssen, J. Nuffer, T. Melz, and H. Hanselka, *J. Am. Ceram. Soc.*, 93 [4] 920–924 (2010).
15. Y. G. Wang, J. Ding, W. Feng, and L. N. An, *J. Am. Ceram. Soc.*, 94 [2] 359–362 (2011).
16. L. Toma, *et al.*, *J. Am. Ceram. Soc.*, 95 [3] 1056–1061 (2012).
17. L. G. Zhang, *et al.*, *J. Am.Ceram. Soc*, 91 [4] 1346–1349 (2008).
18. Y. Li, Y. X. Yu, H. S. San, Y. S. Wang, and L. N. An, *Appl. Phys. Lett.*, 103 163505 (2013).
19. L. Liew, W. G. Zhang, V. M. Bright, L. N. An, M. L. Dunn, and R. Raj, *Sens. Actuators, A*, 89 [1–2] 64–70 (2001).
20. Y. H. Chen, F. Q. Yang, and L. N. An, *Appl. Phys. Lett.*, 102 231902 (2013).
21. M. Birot, J. Pilot, and J. Dunogues, *Chem. Rev.*, 95 [5] 1443–1477 (1995).
22. Y. H. Li, X. D. Li, and D. P. Kim, *J. Electroceram.*, 23 [2–4] 133–136 (2009).
23. Y. S. Wang, T. Jiang, L. G. Zhang, and L. N. An, *J. Am. Ceram. Soc.*, 92 [12] 3111–3113 (2009).
24. B. Doucey, *et al.*, *J. Mater. Sci.*, 37 [13] 2737–2745 (2002).
25. K. B. Sundaram and J. Alizadeh, *Thin Solid Films*, 370 [1–2] 151–154 (2000).
26. E. A. Davis and N. F. Mott, *Phil. Mag.*, 22 [179] 903–922 (1970).
27. Y. G. Wang, K. W. Wang, L. G. Zhang, and L. N. An, *J. Am. Ceram. Soc.*, 94 [10] 3359–3363 (2011).
28. P. O'Connor and J. Tauc, *Solid State Commun.*, 36 [11] 947–949 (1980).
29. J. P. Salvetat, J. M. Bonard, L. Forro, F. Beuneu, and C. IHuillier, *J. Appl. Phys.*, 99 113907 (2006).
30. S. Trassl, G. Motz, E. Rossler, and G. Ziegler, *J. Am. Ceram. Soc.*, 85 [1] 239–244 (2002).
31. B. L. V. Prasad, *et al.*, *Phys. Rev. B*, 62 11209–11218 (2000).
32. I. Menapace, *et al.*, *J. Mater. Sci.*, 43 [17] 5790–5796 (2008).
33. S. Ohnishi, Y. Ikeda, and S. Sugimoto, *J. Polym. Sci. A Polym. Chem.*, 47 [149] 503–507 (1960).